

Precise Localization and Control of Catalytic Janus Micromotors using Weak Magnetic Fields

Regular Paper

Islam S. M. Khalil^{1*}, Veronika Magdanz², Samuel Sanchez^{3,4,5}, Oliver G. Schmidt² and Sarthak Misra^{6,7}

¹ German University in Cairo, New Cairo City, Egypt

² Institute for Integrative Nanosciences, IFW Dresden, Germany

³ Max Planck Institute for Intelligent Systems, Stuttgart, Germany

⁴ Institute for Bioengineering of Catalonia (IBEC), Barcelona, Spain

⁵ Catalan Institution for Research and Advanced Studies (ICREA), Barcelona, Spain

⁶ Department of Biomechanical Engineering, MIRA—Institute for Biomedical Technology and Technical Medicine, University of Twente, Enschede, The Netherlands

⁷ Department of Biomedical Engineering, University of Groningen and University Medical Centre Groningen, The Netherlands

*Corresponding author(s) E-mail: islam.shoukry@guc.edu.eg

Received 12 May 2014; Accepted 10 June 2014

DOI: 10.5772/58873

© 2015 The Author(s). Licensee InTech. This is an open access article distributed under the terms of the Creative Commons Attribution License (<http://creativecommons.org/licenses/by/3.0>), which permits unrestricted use, distribution, and reproduction in any medium, provided the original work is properly cited.

Abstract

We experimentally demonstrate the precise localization of spherical Pt-Silica Janus micromotors (diameter 5 μm) under the influence of controlled magnetic fields. First, we control the motion of the Janus micromotors in two-dimensional (2D) space. The control system achieves precise localization within an average region-of-convergence of 7 μm . Second, we show that these micromotors provide sufficient propulsion force, allowing them to overcome drag and gravitational forces and move both downwards and upwards. This propulsion is studied by moving the micromotors in three-dimensional (3D) space. The micromotors move downwards and upwards at average speeds of 19.1 $\mu\text{m/s}$ and 9.8 $\mu\text{m/s}$, respectively. Moreover, our closed-loop control system achieves localization in 3D space within an average region-of-convergence of 6.3 μm in diameter. The precise motion control and localization of the Janus micromotors in 2D and 3D spaces

provides broad possibilities for nanotechnology applications.

Keywords micromotors, magnetic control, localization, 3D space, self-propulsion

1. Introduction

Self-propelled micromotors demonstrate fully autonomous motion and are attractive devices for various tasks on the microscale. They show promise for diverse biomedical applications, such as targeted drug delivery, cleaning clogged arteries, cell sorting, biopsy [1] and other applications, such as micromanipulation [2], microassembly [3] and microactuation [4]. Magnetic Janus micromotors consist of a platinum-covered hemisphere and a second non-catalytic hemisphere. The platinum cap provides the

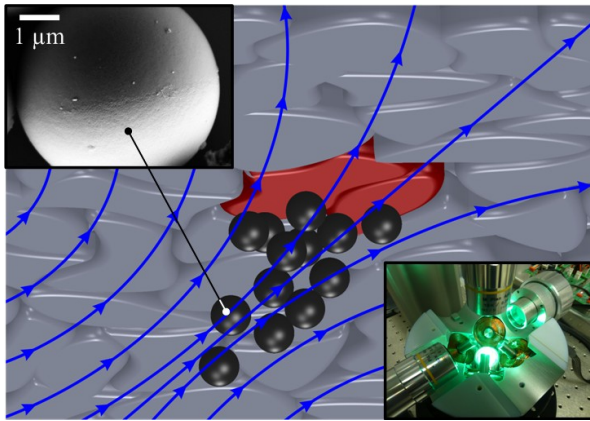


Figure 1. Schematic representation of the autonomous motion of catalytic Janus micromotors ($5\ \mu\text{m}$ in diameter) and steering under the influence of the controlled magnetic fields. The Janus micromotors can be used to achieve targeted drug delivery by controlling their motion in relation to diseased cells (red) so as to decrease negative side-effects on healthy cells (grey). The magnetic fields are generated using the electromagnetic system shown in the bottom-right corner. The inset in the upper-left corner shows a scanning electron microscopy image of a Janus micromotor.

particle with a propulsion force due to the catalysis of hydrogen peroxide to oxygen and water on the platinum surface. In addition to the propulsion feature, the Janus particles possess a magnetic cobalt/platinum multilayer cap underneath the platinum that allows the particle to align its magnetic moment along the main symmetry axis of the cap [5]. This feature provides the Janus micromotor with controlled motion when exposed to an external magnetic field.

Self-driven Janus micromotors have been shown to be useful in several applications, such as DNA hybridization [6], hydrazine detection [7], environmental remediation [8] and micro-cargo delivery [5]. However, there exist at least three challenges that must be overcome before utilization can be made of Janus micromotors in biomedical applications. These challenges are the precise localization and motion control of the Janus micromotors in 2D and 3D spaces [9], the visualization of these micromotors using a clinical imaging modality [10, 11], and their biocompatibility for *in vivo* applications [12].

Controlled magnetic fields have been used to steer and drive self-propelled [13]–[19] and magnetically-driven microrobots [20]–[23]. Baraban et al. have experimentally demonstrated the transportation of colloidal cargoes using single and pairs of Janus micromotors as carriers [24]. It has also been shown that the application of a weak homogeneous magnetic field achieves the directed motion of the Janus micromotors [25]. This motion control has been done in 2D space without feedback to achieve the precise localization that is required for *in vivo* applications.

In this study, we present advances in the motion control of self-driven Janus micromotors in 2D and 3D spaces. We show that the Janus micromotors can be precisely localized using point-to-point motion control. Furthermore, we show that the propulsion force generated using the Janus

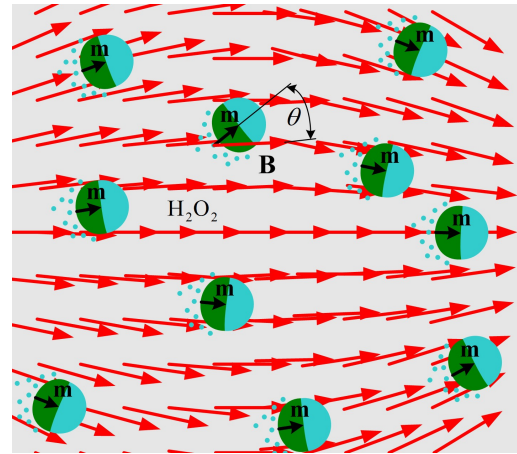


Figure 2. Autonomous motion of the Janus micromotors along the external magnetic field lines (B). The magnetic dipole moment (m) of the Janus micromotor allows for orientation along the field lines, whereas the catalytic decomposition of the hydrogen peroxide (H_2O_2) solution allows for its propulsion. The magnetic torque exerted on the magnetic dipole of the Janus micromotors aligns them along the field lines. The angle between the magnetic dipole and the magnetic field is denoted by θ .

micromotors overcomes drag and gravitational forces, hence allowing them to achieve upwards and downwards controlled motion in relation to a reference position in 3D space.

The remainder of this paper is organized as follows: Section 2 provides descriptions pertaining to the manufacturing, modelling and motion control of the Janus micromotors. The localization and motion control experiments of the Janus micromotors in 2D and 3D spaces are included in Section 3. Finally, Section 4 concludes and provides directions for future work.

2. Fabrication and control of Janus micromotors

The manufacturing of Janus micromotors has been reported by Baraban et al. [5]. They are synthesized using silica colloids (SiO_2) and capped with multiple layers of cobalt/platinum. It has also been reported that these motors move in hydrogen peroxide due to the catalytic decomposition at the platinum surface. The magnetic layer system offers the directional control of the Janus particle when external magnetic fields are applied.

2.1 Fabrication of the Janus micromotors

A suspension of spherical silica colloids (Bangs Laboratories) with a diameter of $5\ \mu\text{m}$ is dropped onto an oxygen-plasma-cleaned $15\ \text{mm} \times 15\ \text{mm}$ glass substrate so that a monolayer of particles forms on the glass slide. The glass slides are dried under ambient conditions to remove the solvent. Afterwards, the glass slides are introduced to the vacuum chamber (base pressure of 1×10^{-7} mbar) of a sputtering machine where the deposition of the magnetic cap consisting of 1 nm platinum, eight alternating layers of 0.3 nm cobalt and 0.8 nm platinum, and a finishing catalytic layer of 5 nm platinum, is carried out as described by

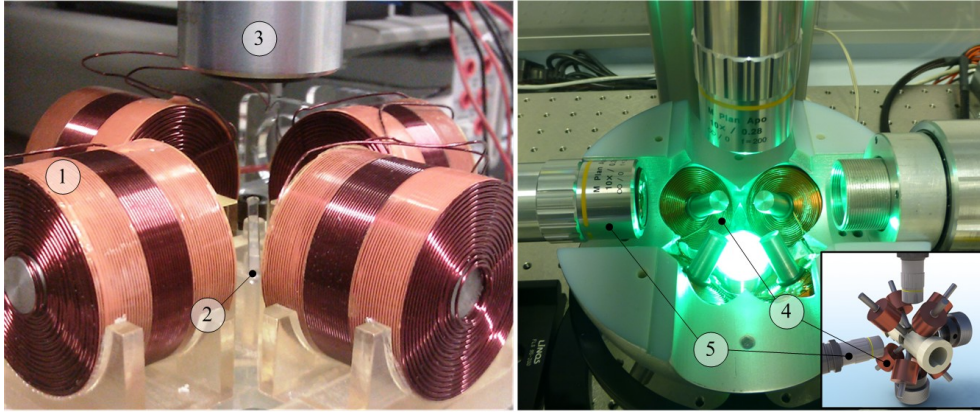


Figure 3. Electromagnetic systems for the motion control of Janus micromotors in 2D and 3D spaces. Left: An electromagnetic system with an orthogonal configuration of coils ① for the 2D motion control of the Janus micromotors using microscopic feedback ② inside a capillary tube ③. Right: An electromagnetic system for 3D motion control inside a capillary tube (not shown). The system consists of eight electromagnetic coils ④ (bottom-right inset) and two microscopic systems ⑤ with auto-focusing.

Baraban et al. [5]. The Janus particles were released from the glass substrate by scratching with tweezers and by dipping the particles in 10% (v/v) hydrogen peroxide solution (in which the experiments were conducted).

2.2 Modelling and control of the Janus micromotors

Under the influence of uniform magnetic fields, the Janus micromotor is subjected to a pure magnetic torque that aligns its magnetic dipole along the field lines. Therefore, the rotational dynamics of the Janus micromotors are given by:

$$|\mathbf{B}| |\mathbf{m}| \sin\theta + \alpha\omega = 0, \quad (1)$$

where \mathbf{B} and \mathbf{m} are the induced magnetic field and the magnetic dipole moment of the Janus micromotor, respectively. Further, θ is the angle between the induced magnetic field and the magnetic dipole moment, as shown in Fig. 2. α and ω are the rotational drag coefficient and the angular velocity of the Janus micromotor, respectively. The first term in (1) allows the Janus micromotors to orient, whereas the catalytic decomposition of the hydrogen peroxide at the platinum surface allows them to move.

Fig. 4 demonstrates experimentally that the motion of the Janus micromotors is only due to their self-propulsive force. At time $t = 0.5$ seconds and before $t = 1.0$ seconds, zero magnetic field is applied. At time $t = 1.0$ seconds, uniform magnetic fields are applied with an orientation towards the first reference position (small blue circle). We observe that the Janus micromotor reverses its direction and moves at the same speed towards the reference position once the magnetic field is applied. The speed of the Janus micromotor is calculated to be $6 \mu\text{m/s}$ before and after the magnetic fields. Therefore, the motion of the Janus micromotor is attributed only to its self-propulsive force.

We also compare the maximum drag force and magnetic force exerted on the Janus micromotor. The drag force (F_d) is calculated to be 1.32×10^{-12} N using:

$$F_d = 6\pi\eta r_p v, \quad (2)$$

where η , r_p and v are the dynamic viscosity of the hydrogen peroxide solution, the radius of the Janus micromotor and its speed, respectively. The magnetic force (\mathbf{F}) exerted on its magnetic dipole is given by [28]-[30]:

$$\mathbf{F} = (\mathbf{m} \cdot \nabla) \mathbf{B}. \quad (3)$$

This magnetic force is generated using two electromagnetic systems for the motion control in 2D and 3D spaces. The 2D electromagnetic system generates a maximum magnetic field gradient of 0.06 T/m [27], whereas the 3D electromagnetic system generates a maximum magnetic field gradient of 1.64 T/m [9]. The upper limit of the magnetic dipole moment of our Janus micromotors is calculated using the volume integral of the saturation magnetization of the cobalt/platinum layers. This upper limit is calculated to be $6.0 \times 10^{-13} \text{ Am}^2$. Therefore, the maximum magnetic force exerted on Janus micromotors using the 2D and 3D electromagnetic systems is $3.60 \times 10^{-14} \text{ N}$ and $9.83 \times 10^{-13} \text{ N}$, respectively. This calculation indicates that the drag force on the Janus micromotors is overcome using its propulsion force (Table 1).

Maximum drag force [N]	1.32×10^{-12}
Maximum magnetic force in 2D [N]	3.60×10^{-14}
Maximum magnetic force in 3D [N]	9.83×10^{-13}

Table 1. Maximum drag and magnetic forces on the Janus micromotors. The drag force is calculated using a speed of $14 \mu\text{m/s}$. The magnetic forces in 2D and 3D are calculated using magnetic field gradients of 0.06 T/m and 1.64 T/m , respectively. The drag and magnetic forces are calculated using (2) and (3).

Motion control of the Janus micromotors is achieved in 2D and 3D spaces by orienting the magnetic field lines towards the reference position. The magnetic field lines are controlled based on the position of the Janus micromotor with

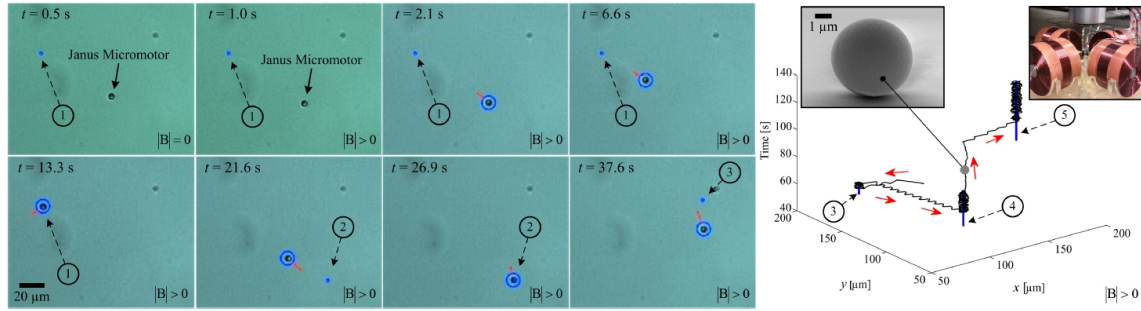


Figure 4. A representative closed-loop motion control result of a Janus micromotor (diameter of 5 μm). Before time $t = 1$ seconds, no magnetic fields are applied and the Janus micromotors move using their propulsive force. The Janus micromotors move at a speed of 6 $\mu\text{m/s}$. At time $t = 1$ seconds, magnetic fields are applied to orient the Janus micromotors towards the first reference position ①. The Janus micromotors reverse their direction and moves towards the reference position (at the same speed) once the magnetic fields are applied. The right figure shows the localization of the Janus micromotors within the vicinity of three reference positions (vertical blue lines represent the position references ③, ④ and ⑤).

respect to the reference position [9, 20]. This control is designed using (3) by devising a desired magnetic force that points towards the reference position:

$$\mathbf{K}_D \dot{\mathbf{e}} + \mathbf{K}_P \mathbf{e} = (\mathbf{m} \cdot \nabla) \tilde{\mathbf{B}} \mathbf{I}, \quad (4)$$

where \mathbf{e} and $\dot{\mathbf{e}}$ are the position-tracking error and velocity of the Janus micromotors (reference position is fixed), respectively. Further, \mathbf{K}_D and \mathbf{K}_P are positive-definite gain matrices, and $\tilde{\mathbf{B}}$ is a constant matrix that maps the current input (\mathbf{I}) onto magnetic fields. The matrices \mathbf{K}_D and \mathbf{K}_P must be selected such that $(6\pi\eta r_p \Pi + \mathbf{K}_D)^{-1} \mathbf{K}_P$ is positive-definite [27], where Π is the identity matrix. Solving (4) for the current vector allows us to control the magnetic fields towards a reference position [26, 27]. This control is achieved using (4), since the magnetic force lines have the same direction as the magnetic field lines within the workspace of our magnetic systems [26]. Therefore, (4) allows us to control the direction of the Janus micromotor towards the reference position.

3. Localization of the Janus micromotors

The motion control of the Janus micromotors is achieved using two electromagnetic systems. A 2D electromagnetic system is used to achieve the planar manipulation of the Janus micromotor, whereas a 3D electromagnetic system is used to demonstrate that the Janus micromotors can overcome the gravitational force and move upwards and downwards. Characteristics of these magnetic systems are provided in Table 2. In these experiments, the Janus micromotors are contained inside capillary tubes (Vitro-Com, VitroTubes 3520-050, Mountain Lakes, USA) with a 10% (v/v) hydrogen peroxide solution.

3.1 Localization of the Janus micromotors in 2D space

An electromagnetic system (inset in Fig. 4) with an orthogonal configuration of four electromagnetic coils is used to manipulate the Janus micromotors in 2D space. Fig. 4 shows a representative motion control result of a Janus

micromotor towards five reference positions. The controlled magnetic fields are applied after $t = 1$ seconds. At this time instant, the Janus micromotor reverses its direction and moves towards the reference position at the same speed (6 $\mu\text{m/s}$). We repeated this experiment five times, and the average speed is calculated as $13 \pm 7 \mu\text{m/s}$. Further, due to the self-propulsive force of the Janus micromotors, our closed-loop control system localizes the Janus micromotors within the vicinity of the reference position, as shown in Fig. 4. The localization is evaluated using the area in which the Janus micromotors are localized. This area is defined as a region of convergence (ROC). The average ROC is calculated as $7 \pm 1.5 \mu\text{m}$.

3.2 Localization of the Janus micromotors in 3D space

Full autonomous motion in 3D space is demonstrated for the Janus micromotors using an electromagnetic system with eight electromagnetic coils (inset in Fig. 5). The Janus micromotors are contained inside a capillary tube within the centre of the electromagnetic system. The eight electromagnetic coils allow for the orienting of the Janus micromotor in all directions in 3D. The average speed along the x -, y - and z -axis are calculated as 14.5 $\mu\text{m/s}$, 14.0 $\mu\text{m/s}$ and 14.4 $\mu\text{m/s}$, respectively. Further, we observe that the Janus micromotors move downwards and upwards at average speeds of 19.1 $\mu\text{m/s}$ and 9.8 $\mu\text{m/s}$, respectively. The closed-loop control in 3D space allows us to localize the Janus micromotors within a ROC of 6.3 μm .

The x and y velocity components of the Janus micromotor in 3D space indicate that the motion of the Janus micromotor is due to its propulsion force. These components provide an average speed of 14.2 $\mu\text{m/s}$ using the 3D magnetic system, as opposed to 13.6 $\mu\text{m/s}$ using the 2D magnetic system. The slight increase in the average speed is due to the magnetic field gradient generated using the 3D magnetic system (1.64 T/m), which is approximately 27 times greater than that (0.06 T/m) generated using the 2D magnetic system. Therefore, the motion of the Janus micromotors depends mainly on their self-propulsive force.

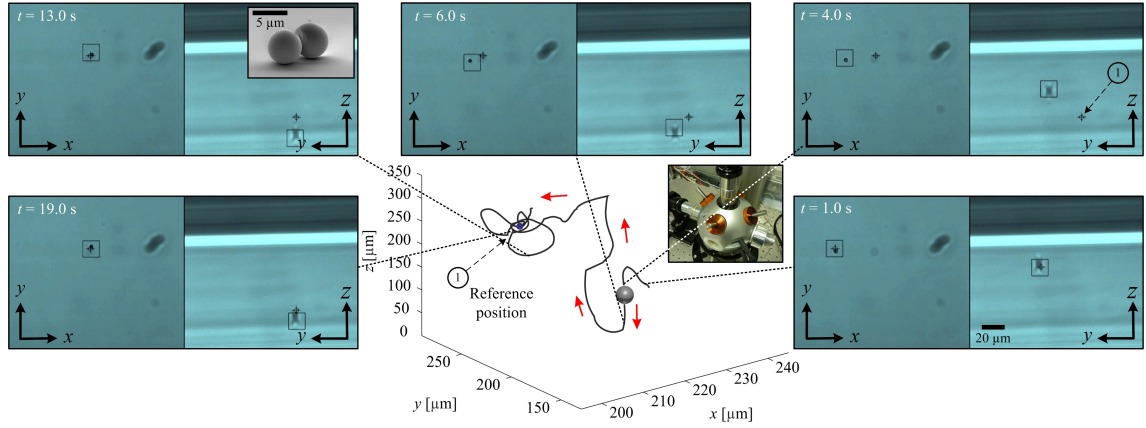


Figure 5. A representative closed-loop motion control result of a Janus micromotor (diameter of 5 μm) in 3D space. Motion control is accomplished in 3D space using the electromagnetic system shown in the inset. The Janus micromotor is contained inside a capillary tube within the centre of the electromagnetic system. After $t = 1$ seconds, a reference position ① is given. The reference position is shown in the xy - and yz -views using a cross-hair. The black square indicates the Janus micromotor and is assigned using our feature-tracking algorithm.

In these experiments, the concentration of the H_2O_2 used for the propulsion of the Janus micromotors is beyond biocompatible limits. At 0.25% H_2O_2 , mammalian cells have been shown to be viable only for 30 minutes [31]. Researchers are trying to tackle the challenge of the biocompatibility of the fuel in order to achieve real biomedical applications. Once an alternative fuel is provided, it could either be taken from the body fluid or injected together with the Janus micromotors.

4. Conclusions

The autonomous motion of Janus micromotors in 2D and 3D spaces is demonstrated experimentally using two electromagnetic systems that generate relatively weak (0.06 T/m) and strong (1.64 T/m) magnetic field gradients. We observe that using a relatively large magnetic field gradient results in a slight increase in the planar components of the velocity vector of the Janus micromotor. Therefore, the motion of the Janus micromotors is attributed to the propulsion force that is generated due to the catalytic decomposition of H_2O_2 . Moreover, we show the automatic control of the Janus micromotors in 2D and 3D spaces, which allows us to achieve precise localization within the vicinity of the reference positions.

Parameter	Value	Parameter	Value
$\max I_i [\text{A}]$	1.0	Workspace [mm^2]	2.4×1.8
$ B [\text{mT}]$	15	$\nabla B [\text{mT}^{-1}]$	0.06
Coils	4	Frame per second	15
$\max I_i [\text{A}]$	2.0	Workspace [mm^3]	$10 \times 10 \times 10$
$ B [\text{mT}]$	85	$\nabla B [\text{mT}^{-1}]$	1.64
Coils	8	Frame per second	120

Table 2. Characteristics of the 2D and 3D magnetic systems. I_i is the current at the i th coil, and ($i = 1, \dots, 4$) and ($i = 1, \dots, 8$) for the 2D and 3D magnetic systems, respectively.

5. Acknowledgements

The authors acknowledge the funding from MIRA-Institute for Biomedical Technology and Technical Medicine, University of Twente. The research leading to these results has also received funding from the European Research Council under the European Union's Seventh Framework Programme (FP7/2007-2013)/ERC grant agreement no. 311529.

The authors thank Mr. Bart A. Reefman for collecting the data used in Figs. 4 and 5. They would also like to thank Mrs. C. Krien for sputtering and Dr. M. Guix for assistance with the SEM imaging.

6. References

- [1] Q. A. Pankhurst, J. Connolly, S. K. Jones, and J. Dobson, "Applications of magnetic nanoparticles in biomedicine," *Journal of Physics*, Vol. 36, no. 13, pp. 167-181, July 2003.
- [2] S. Martel and M. Mohammadi, "Using a swarm of self-propelled natural microrobots in the form of flagellated bacteria to perform complex micro-assembly tasks," in *Proceedings of the IEEE International Conference on Robotics and Automation (ICRA)*, pp. 500-505, Alaska, USA, May 2010.
- [3] S. Martel, "Controlled bacterial micro-actuation," in *Proceedings of the International Conference on Microtechnologies in Medicine and Biology*, pp. 89-92, Okinawa, Japan, May 2006.
- [4] S. Sanchez, A. A. Solovev, S. Schulze, and O. G. Schmidt, "Controlled manipulation of multiple cells using catalytic microbots," *Chemical Communication*, vol. 47, pp. 698-700, November 2010.
- [5] L. Baraban, D. Makarov, R. Streubel, I. Mönch, D. Grimm, S. Sanchez, and O. G. Schmidt, "Catalytic Janus motors on microfluidic chip: deterministic

- motion for targeted cargo delivery," *ACS Nano*, vol. 6, no. 4, pp. 3383-3389, March 2012.
- [6] J. Simmchen, A. Baeza, D. Ruiz, M. J. Esplandiú, and M. Vallet-Regí, "Asymmetric hybrid silica nanomotors for capture and cargo transport: towards a novel motion-based DNA sensor," *Small*, vol. 8, no. 13, pp. 2053-2059, July 2012.
 - [7] W. Gao, A. Pei, R. Dong, and J. Wang, "Catalytic iridium-based Janus micromotors powered by ultralow levels of chemical fuels," *Journal of the American Chemical Society*, vol. 136, no. 6, pp. 2276-2279, January 2014.
 - [8] W. Gao, X. Feng, A. Pei, Y. Gu, J. Lia, and J. Wang, "Seawater-driven magnesium based Janus micromotors for environmental remediation," *Nanoscale*, vol. 5, no. 11, pp. 4696-4700, January 2013.
 - [9] I. S. M. Khalil, V. Magdanz, S. Sanchez, O. G. Schmidt, and S. Misra, "Three-dimensional closed-loop control of self-propelled microjets," *Applied Physics Letters*, 103, 172404, October 2013.
 - [10] S. Martel, O. Felfoul, J.-B. Mathieu, A. Chanu, S. Tamaz, M. Mohammadi, M. Mankiewicz, and N. Tabatabaei, "MRI-based medical nanorobotic platform for the control of magnetic nanoparticles and flagellated bacteria for target interventions in human capillaries," *International Journal of Robotics Research*, vol. 28, no. 9, pp. 1169-1182, September 2009.
 - [11] I. S. M. Khalil, P. Ferreira, R. Eleutério, C. L. de Korte, and S. Misra, "Magnetic-Based closed-loop control of paramagnetic microparticles using ultrasound feedback," in *Proceedings of the IEEE International Conference on Robotics and Automation (ICRA)*, pp. 3807-3812, Hong Kong, China, June 2014.
 - [12] H. Jaganathan and B. Godin, "Biocompatibility assessment of Si-based nano-and micro-particles" *Advanced Drug Delivery Reviews* 64, (2012) 1800-1819
 - [13] W. F. Paxton, K. C. Kistler, C. C. Olmeda, A. Sen, St. Angelo SK, Y. Cao, T. E. Mallouk, P. E. Lammert, and V. H. Crespi (2004) Catalytic nanomotors: autonomous movement of striped nanorods. *Journal of the American Chemical Society*. 126: 13424-13431.
 - [14] S. Fournier-Bidoz, A. C. Arsenault, I. Manners, and G. A. Ozin, Synthetic self-propelled nanorotors. *Chemical Communication*. vol. 441, pp. 441-443, 2004.
 - [15] J. R. Howse, R. A. L. Jones, A. J. Ryan, T. Gough, R. Vafabakhsh, and R. Golestanian, Self-Motile colloidal particles: from directed propulsion to random walk. *Physical Review Letters*. vol. 99 (048102), 2007.
 - [16] Y. F. Mei, G. Huang, A. A. Solovev, E. B. Urena, I. Monch, F. Ding, T. Reindl, R. K. Y. Fu, P. K. Chu, and O. G. Schmidt, Versatile approach for integrative and functionalized tubes by strain engineering of nanomembranes on polymers. *Advanced Materials*, vol. 20, pp. 4085-4090, 2008.
 - [17] A. A. Solovev, Y. F. Mei, E. B. Urena, G. Huang, and O. G. Schmidt, Catalytic microtubular jet engines self-propelled by accumulated gas bubbles. *Small*, vol. 5, pp. 1688-1692, 2009.
 - [18] L. Zhang, J. J. Abbott, L. Dong, B. E. Kratochvil, D. Bell, and B. J. Nelson, Artificial bacterial flagella: fabrication and magnetic control. *Applied Physics Letters*. 94: 064107, 2009.
 - [19] A. Ghosh and P. Fischer, Controlled propulsion of artificial magnetic nanostructured propellers. *Nano Letters*. 9: 2243-2245, 2009.
 - [20] M. P. Kummer, J. J. Abbott, B. E. Kratochvil, R. Borer, A. Sengul, and B. J. Nelson, "OctoMag: an electromagnetic system for 5-DOF wireless micromanipulation," *IEEE Transactions on Robotics*, vol. 26, no. 6, pp. 1006-1017, December 2010.
 - [21] S. Floyd, C. Pawashe and M. Sitti, "Two-dimensional contact and noncontact micromanipulation in liquid using an untethered mobile magnetic microrobot," *IEEE Transactions on Robotics*, vol. 25, no. 6, pp. 1332-1342, December 2009.
 - [22] C. Pawashe, S. Floyd, E. Diller and M. Sitti, "Two-dimensional autonomous microparticle manipulation strategies for magnetic microrobots in fluidic environments," *IEEE Transactions on Robotics*, vol. 28, no. 2, pp. 467-477, April 2012.
 - [23] K. E. Peyer, L. Zhang, B. J. Nelson, "Bio-inspired magnetic swimming microrobots for biomedical applications," *Nanoscale*, vol. 5, pp. 1259-1272, November 2012.
 - [24] L. Baraban, M. Tasinkevych, M. N. Popescu, S. Sanchez, S. Dietrich and O. G. Schmidt, "Transport of cargo by catalytic Janus micro-motors," *Soft Matter*, vol. 48, no. 8, pp. 48-52, February 2012.
 - [25] L. Baraban, D. Makarov, O. G. Schmidt, G. Cuni-berti, P. Leiderere and A. Erbef, "Control over Janus micromotors by the strength of a magnetic field," *Nanoscale*, vol. 5, pp. 1332-1336, 2013.
 - [26] I. S. M. Khalil, V. Magdanz, S. Sanchez, O. G. Schmidt, and S. Misra, "The control of self-propelled microjets inside a microchannel with time-varying flow rates," *IEEE Transactions on Robotics*, vol. 30, no. 1, pp. 49-58, February 2014.
 - [27] I. S. M. Khalil, M. P. Pichel, L. Abelmann, and S. Misra, "Closed-loop control of magnetotactic bacteria," *The International Journal of Robotics Research*, vol. 32, no. 6, pp. 637-649, May 2013.
 - [28] D. Jiles, "Introduction to magnetism and magnetic materials", Taylor & Francis, 1998.
 - [29] T. H. Boyer, "The force on a magnetic dipole," *American Journal of Physics*, vol. 56, no. 8, pp. 688-692, August 1988.

- [30] S. S. Shevkoplyas, A. C. Siegel, R. M. Westervelt, M. G. Prentiss, and G. M. Whitesides, "The force acting on a super paramagnetic bead due to an applied magnetic field," *Lab on a Chip*, vol. 7, no. 6, pp. 1294-1302, July 2007.
- [31] S. Sanchez, A. N. Ananth, V. M. Fomin, M. Viehrig, and O. G. Schmidt, "Superfast motion of catalytic microjet engines at physiological temperature," *Journal of the American Chemical Society*, vol. 133, no. 38, pp. 14860-14863, August 2011.